DESY 17-055, FERMILAB-PUB-17-077-T, LAPTh-009/17, MIT-CTP-4898

Supplementary Material: Probing new light force-mediators by isotope shift spectroscopy

Julian C. Berengut,[1] Dmitry Budker,[2,3,4] Cédric Delaunay,[5] Victor V. Flambaum,[1] Claudia Frugiuele,[6] Elina Fuchs,[6] Christophe Grojean,[7,8] Roni Harnik,[9] Roee Ozeri,[10] Gilad Perez,[6] and Yotam Soreq[11]

[1] *School of Physics, University of New South Wales, Sydney, New South Wales 2052, Australia*
[2] *Helmholtz-Institut Mainz, Johannes Gutenberg-Universität Mainz, 55128 Mainz, Germany*
[3] *Physics Department, University of California, Berkeley 94720-7300, USA*
[4] *Nuclear Science Division, Lawrence Berkeley National Laboratory, Berkeley, California 94720, USA*
[5] *Laboratoire d'Annecy-le-Vieux de Physique Théorique LAPTh, CNRS – Université Savoie Mont Blanc, BP 110, F-74941 Annecy-le-Vieux, France*
[6] *Department of Particle Physics and Astrophysics, Weizmann Institute of Science, Rehovot 7610001, Israel*
[7] *DESY, D-22607 Hamburg, Germany*
[8] *Institut für Physik, Humboldt-Universität zu Berlin, D-12489 Berlin, Germany*
[9] *Theoretical Physics Department, Fermi National Accelerator Laboratory, Batavia, IL 60510 USA*
[10] *Department of Physics of Complex Systems, Weizmann Institute of Science, Rehovot 7610001, Israel*
[11] *Center for Theoretical Physics, Massachusetts Institute of Technology, Cambridge, MA 02139*

I. VISUALIZING THE VECTOR SPACE

In the main text we define the following vectors in the A' vector space

$$\overrightarrow{m\nu}_i \equiv \left(m\nu_i^{AA'_1}, m\nu_i^{AA'_2}, m\nu_i^{AA'_3}\right) , \tag{S1}$$

$$\overrightarrow{m\delta\langle r^2\rangle} \equiv \left(\langle r^2\rangle_{AA'_1}/\mu_{AA'_1}, \langle r^2\rangle_{AA'_2}/\mu_{AA'_2}, \langle r^2\rangle_{AA'_3}/\mu_{AA'_3}\right) , \tag{S2}$$

$$\overrightarrow{m\mu} \equiv (1,1,1) . \tag{S3}$$

As long as $\overrightarrow{m\nu}_{1,2}$ are spanned by $\overrightarrow{m\mu}$ and $\overrightarrow{m\delta\langle r^2\rangle}$, the resulting King plot will be linear. In Fig. S1, we illustrate the vector space of the various components related to isotope shifts that leads to the nonlinearites. The NP contribution to IS, $\alpha_{\rm NP}X_i\vec{h}$, may lift the IS vectors from the $(\overrightarrow{m\mu}, \overrightarrow{m\delta\langle r^2\rangle})$ plane, resulting in a nonlinear King plot. Figure S2 illustrates a nonlinear King plot, where the area of the triangle corresponds to the NL mentioned in the main text.

II. DERIVATION OF X_i IN THE $m_\phi \to 0$ LIMIT

Here we estimate the NP contribution X_i to IS in the special case where the force-carrier is much lighter than the inverse atomic size, $m_\phi \ll (1+n_e)/a_0 \sim \mathcal{O}(\text{few keV})$. Since in this limit the effective potential is Coulomb-like,

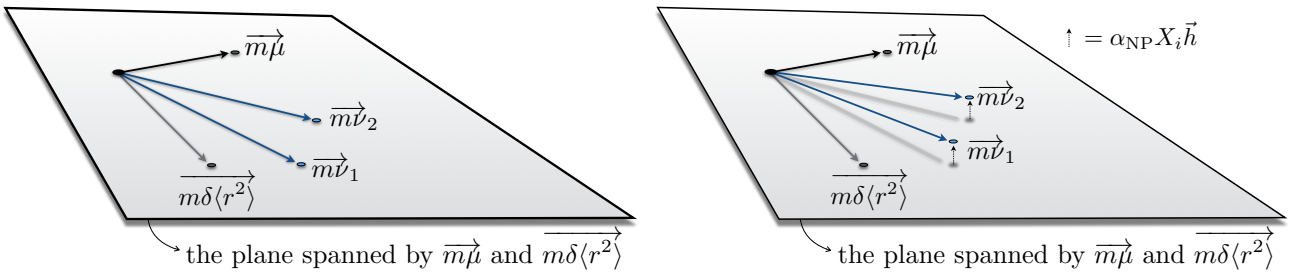

FIG. S1: Left: A cartoon of the prediction of factorization in vector language. All of the isotope shift measurements (which are here three-dimensional vectors $\overrightarrow{m\nu}_{1,2}$) lie in the plane that is spanned by $\overrightarrow{m\mu}$ and $\overrightarrow{m\delta\langle r^2\rangle}$. This coplanarity can be tested by measuring whether $\overrightarrow{m\nu}_1$, $\overrightarrow{m\nu}_2$ and $\overrightarrow{m\mu}$ are coplanar. Right: In the presence of new physics the isotope shift get a contribution which can point out of the plane. A new long-range force can spoil the coplanarity of $\overrightarrow{m\nu}_1$, $\overrightarrow{m\nu}_2$ and $\overrightarrow{m\mu}$.

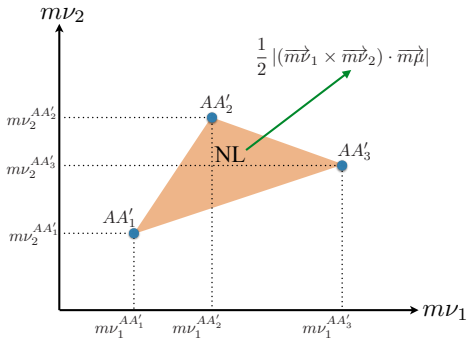

FIG. S2: Illustration of nonlinearity in the King plot of the isotope shifts $\overrightarrow{m\nu}_{1,2}$ in isotope pairs $AA'_j, j = 1, 2, 3$. The area of the triangle corresponds to the NL defined in the main text.

$V_\phi(r) \simeq (A-Z)\alpha_{\rm NP}/r$, X_i can be simply estimated through a shift of the fine-structure constant α, without a detailed calculation of the electronic wavefunctions. At fundamental level, the Coulomb potential is modified by the shift

$$\alpha Z \to \alpha Z + \alpha_{\rm NP}(A - Z)\,. \tag{S4}$$

In the absence of NP, the binding energy of the atomic level a for isotope A scales as

$$E_a^A = (\alpha Z_{\rm eff}^a)^2 I_a^A\,, \tag{S5}$$

where $Z_{\rm eff}^a \equiv Z - \sigma_a$ is the effective nuclear charge seen by the valence electron in the state a, and I_a^A is a constant independent of the charge (modulo $\mathcal{O}(\alpha Z_{\rm eff}^a)^4$ corrections from the fine-structure). The constant $\sigma_a > 0$ accounts for the screening due to inner electrons. A similar screening effect may occur for the new physics force such that Eq. S4 implies to shift the physical observables as

$$\alpha Z_{\rm eff}^a \to \alpha Z_{\rm eff}^a + \alpha_{\rm NP}(A - Z - \sigma'_a)\,, \tag{S6}$$

where the constant σ'_a accounts for the screening of the nuclear NP charge by inner electrons. Note that precise knowledge of this constant is not crucial since it is universal (as a first approximation) for all isotopes and will therefore cancel in X_i.

Hence the prediction for the IS of the transition $i = a \to b$ is (in natural units, i.e. the reduced Planck constant is set to $\hbar = 1$)

$$\begin{aligned}\nu_i^{AA'} =& (E_b^A - E_a^A) - (E_b^{A'} - E_a^{A'}) \\ =& \left[\alpha Z_{\rm eff}^b + \alpha_{\rm NP}(A - Z - \sigma'_b)\right]^2 I_b^A - \left[\alpha Z_{\rm eff}^a + \alpha_{\rm NP}(A - Z - \sigma'_a)^2\right] I_a^A\big] - (A \to A')\,,\end{aligned} \tag{S7}$$

and expanding to leading order in $\alpha_{\rm NP} \ll \alpha$ yields

$$\nu_i^{AA'} \approx \nu_i^{AA'}\big|_{\alpha_{\rm NP}=0} + \frac{2\alpha_{\rm NP}}{\alpha}\left[A\left(\frac{E_b^A}{Z_{\rm eff}^b} - \frac{E_a^A}{Z_{\rm eff}^a}\right) - (A \to A')\right]\,. \tag{S8}$$

Since IS are typically orders of magnitude smaller than the transition frequencies (with the exceptions of very degenerate states such as in dysprosium [1, 2]), we can take $E^{A'} \approx E^A$ in the NP contribution above, and matching to the NP term of $\nu_i^{AA'}$ as given in the main text we find $\gamma_{AA'} = A - A'$ and

$$X_i|_{m_\phi=0} \approx 2\alpha^{-1}\left(\frac{E_b}{Z_{\rm eff}^b} - \frac{E_a}{Z_{\rm eff}^a}\right)\,. \tag{S9}$$

By a combination with the expression for $\alpha_{\rm NP}$, the above expression provides an estimate of the constraint on $\alpha_{\rm NP}$ without the need for an accurate knowledge of electronic densities. For example, we found that the upper bounds on $y_e y_n$ obtained by evaluating X_i with Eq. (S9) and with the CI+MBPT method are comparable and only differ by $\mathcal{O}(1)$ factors.

III. CALCULATION OF THE NP ELECTRONIC COEFFICIENT

To calculate the effect of this NP potential on atomic energies we use the "finite field" method where the potential is added directly to the Dirac equation in the many-body computations. The atomic structure calculations are variants of the combination of configuration interaction and many-body perturbation theory (CI+MBPT) [3]. For the single-valence electron ions Ca^+ and Sr^+, we create an operator $\hat{\Sigma}$ (see for example [4]) representing core-valence correlations to second order in the residual Coulomb interaction. This operator is added to the Dirac-Fock operator, along with the NP potential, to generate self-consistent solutions. In this approach, the sensitivity of a transition i between electronic states a and b can be expressed as

$$X_i = \frac{1}{A-Z}\left.\frac{d\epsilon_{ab}}{d\alpha_{\rm NP}}\right|_{\alpha_{\rm NP}=0}, \tag{S10}$$

where ϵ_{ab} is the difference of the energy levels of the states $a,\ b$, evaluated as a function of $\alpha_{\rm NP}$ and the derivative is taken numerically at $\alpha_{\rm NP}=0$.

For neutral Sr, which has two valence electrons above closed shells, we use the CI+MBPT method as described in [5]. Briefly, we find the self-consistent solution of the Dirac-Fock equations, including the NP potential, for the closed-shell core (i.e. the V^{N_e-2} potential where N_e is the total number of electrons). In this potential we generate a set of B splines [6, 7] which form a complete basis set. Valence-valence correlations are included to all orders using CI, while the core-valence correlations are included using second-order MBPT to modify the radial integrals. The Yb^+ case is more complicated because of the hole transition, $4f^{14}\,6s \to 4f^{13}\,6s^2$. For this ion we use the particle-hole CI+MBPT method in the V^{N_e-1} potential [8] which has previously been used for Hg^+.

The many-body calculations can be cross-checked by perturbation theory, which yields

$$X_i = \int d^3r \frac{e^{-m_\phi r}}{r}\left[|\Psi_b(r)|^2 - |\Psi_a(r)|^2\right], \tag{S11}$$

where $|\Psi(r)|^2$ is the electron-density evaluated in the absence of NP. We use `GRASP2K` [9] to evaluate $|\Psi(r)|^2$ and compute X_i using Eq. (S11) for several Ca^+ transitions. We find good agreement between the two methods.

IV. PROJECTING FUTURE BOUNDS

Our procedure above applies to cases with enough experimental data. For systems lacking (sufficiently precise) measurements, we can still derive projections provided that an acceptable estimation of the F_{21} constant is available from either theory calculation or hyperfine splitting data (whenever available). Assuming the observation of linearity and global experimental uncertainties σ_i of $\nu_i^{AA'}$, the only missing information is how much the new physics vector, $\vec{h}$, points towards the linearity plane. While a precise determination of the vector component requires data, the projection of the NP vector $h_{AA'} = AA'$ amu along the mass shift direction is easily obtained without the need of experimental input. Therefore, a best-case projection[1] $[\sigma_{\alpha_{\rm NP}}]_{\rm proj}$ can be obtained by neglecting the possible additional alignment of NP with nuclear effects,

$$[\sigma_{\alpha_{\rm NP}}]_{\rm proj} \sim \frac{\sqrt{\sigma_2^2+\sigma_1^2F_{21}^2}}{(X_2-X_1F_{21})}\frac{A}{\Delta A_j^{\rm min}\Delta A_j^{\rm max}}, \tag{S12}$$

where $\Delta A_j^{\rm min(max)} \equiv \min\,(\max)[A-A_j]$ and σ_i is the assumed standard deviation of IS measurements in transition i. Note that the sensitivity to $\alpha_{\rm NP}$ is weaker by a factor of $A/\Delta A_j^{\rm min}$ than the naive expectation in the first version of Ref. [10]. The reason is that the NP physics vector lies mostly in the linearity plane, in particular it has a large projection along the mass shift direction. Eq. (S12) implies that elements with small $A/(\Delta A_j^{\rm min}\Delta A_j^{\rm max})$ are preferred. However, if the mass shift dominates over the field shift, which is the case for light elements, the sensitivity is reduced as well.

---

[1] The actual bound obtained by data will be always weaker, $[\sigma\alpha_{\rm NP}]_{\rm proj} \le [\sigma\alpha_{\rm NP}]_{\rm data}$ since the projection neglects the alignment with the FS that will weaken the bound.

V. SCALING OF HIGH-MASS LIMITS

As discussed in the main text, King linearity (or coplanarity) is only sensitive as a probe of long-range forces, which extend beyond the nuclear size. This is because the contribution of a short-range interaction to the isotope shift can be absorbed into the contact interactions such as the nuclear charge radius. From the perspective of an atom, a new interaction approaches essentially a contact interaction when its range is shorter than the effective radius of the innermost K-shell electron, $(Z\alpha m_e)^{-1} = a_0/Z$. We thus expect our method to lose power for mediators heavier than $Z\alpha m_e$.

It is instructive to investigate like what power of $m_\phi/(Z\alpha m_e)$ one would expect the limits to decrease. As shown in the discussion of King linearity, the contribution of NP to nonlinearity is proportional to $(X_2 - X_1 F_{21})$. When the NP contribution is aligned with the FS, $X_i \propto F_i$, this factor vanishes. We must thus investigate how X_i and F_i differ for the various transitions in the limit of $m_\phi \to \infty$. In our proposed procedure, F_i is measured from data and X_i is estimated from theory, leading to the presented limits. Since these two quantities are extracted using different methods we would like to ensure that the alignment of X_i and F_i is captured correctly and that the weakening of the bounds for $m_\phi > Z\alpha m_e$ agrees with our theoretical expectation.

The asymptotic behavior of the limits exhibits an approximate m_ϕ^3 behavior. We will now show that this may be expected on theoretical grounds, first in position space, using a hydrogen-like approximation and then in momentum space, using an effective field theory (EFT).

To leading order in the small new physics coupling, the contribution of a new Yukawa potential to the energy of the atomic level a is

$$\Delta E_a = \alpha_{\rm NP} \int d^3r \frac{e^{-m_\phi r}}{r} |\Psi_a(r)|^2 \ . \tag{S13}$$

To study the scaling behavior in a simple case, we approximate the multi-electron crudely as a single-electron atom with an effective $Z_{\rm eff}^{(a)}$ which will account for the screening of the nucleus by the inner shells. Clearly, the full calculation of X_i accounts for the multi-electron effects fully and the approximation we use here should be taken as a toy model to study the scaling of our bounds. We consider atoms in the nS state, with $(n = 1, 2, \ldots)$, which is relevant for us since many of our isotope shifts involve an S state. Using the explicit form of non-relativistic hydrogen-like wavefunctions, it is simple to show that in this case

$$\Delta E_{n\rm S} = \alpha_{\rm NP} \frac{|\psi_{n\rm S}(0)|^2}{m_\phi^2} \left(1 - \frac{4 Z_{\rm eff}^{(n\rm S)} \alpha\, m_e}{m_\phi} + \ldots\right) , \tag{S14}$$

where we assumed that $m_\phi \gg Z\alpha m_e$ and expanded in powers of $1/m_\phi$, keeping the first two terms. The leading term is to be expected, and is identical to the shift in energy from a contact interaction potential $\delta^3(r)/m_\phi^2$. This term will thus lead to isotope shifts in the $a \to b$ transition that are proportional to $|\Psi_a(0)|^2 - |\Psi_b(0)|^2$ and thus proportional to the FS. This term therefore cancels in the combination $(X_2 - X_1 F_{21})$. The second term in Eq. (S14) has an additional factor of $Z_{\rm eff}$ leading to an IS proportional to $Z_{\rm eff}^{(a)} |\Psi_a(0)|^2 - Z_{\rm eff}^{(b)} |\Psi_b(0)|^2$. This term will not cancel in $(X_2 - X_1 F_{21})$, and since it scales as m_ϕ^{-3} we would expect the bounds to lose power as m_ϕ^3 at high mass[2].

We can also understand the scaling of our bounds at high mediator mass in an EFT, where the heavy mediator was integrated out. The appropriate EFT for this purpose is known as non-relativistic QED (NRQED) [11]. This EFT is often used to study nuclear effects in atoms, but here we will use it to describe our heavy mediator. In this theory the effects of the heavy mediator are captured by four-fermion interactions suppressed by powers of m_ϕ. The reader who is familiar with NRQED may be surprised by the m_ϕ^{-3} because the theory contains four-fermion operators that are suppressed by m_ϕ^{-2} and by m_ϕ^{-4} but none that are suppressed by a cubic power [12]. This however can be resolved within NRQED as we now show, since the m_ϕ^{-3} is simply a 1-loop correction to the m_ϕ^{-2} Wilson coefficient[3].

To demonstrate the m_ϕ^{-3} scaling one needs to do a 1-loop matching between the full Yukawa theory and the EFT. This calculation amounts to calculating the LO QED correction to the tree level calculation in the Yukawa theory. To perform the matching we calculate a physical quantity twice, once in the full theory and once in the EFT, and then set the Wilson coefficient in the EFT to get a similar result order by order in perturbation theory. For the full

---

[2] It is interesting to note, that for a single electron atom, where $Z_{\rm eff} = Z$ for all states, the isotope shift again scales as $|\Psi_a(0)|^2 - |\Psi_b(0)|^2$. In this case the bound will scale as m_ϕ^4 from the higher order terms that were dropped in Eq. (S14).

[3] We thank Richard Hill for an enlightening conversation.

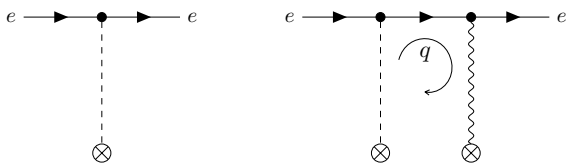

FIG. S3: Feynman diagrams for the two point function of the electron in the presence of a nucleus. We take external momenta to zero. The tree level diagram is the first correction of the Yukawa potential and the loop calculation is the first QED correction to it. The position-space calculation uses the full hydrogen wavefunction and thus effectively re-sums all such corrections with an arbitrary number of photon exchanges.

theory we take non-relativistic QED with an additional Yukawa interaction. For simplicity we take the nucleus to be infinitely heavy and of zero size. The nuclear charge will again be set to $Z_{\rm eff}$, in accordance with the approximation taken above for electron screening effects. The Yukawa propagator in momentum space is $(q^2+m_\phi^2)^{-1}$ and the rest of the Feynman rules are shown in [13].

The EFT we will match onto is NRQED, again with an infinitely heavy nucleus, but with the inclusion of one contact interaction between the nucleus, N, and the electron $C(\psi_e^*\psi_e)(\psi_N^*\psi_N)/m_\phi^2$, where C is a Wilson coefficient. Since we are only interested in the scaling behavior we will not dwell on precise numerical coefficients, but will focus on the parametric scaling. A quantity that is simple to compute for this matching calculation is the two-electron correlation function setting external momenta to zero, thus avoiding complications of bound states.

We begin by matching at tree level. In the full theory, to LO in the NP interaction, the tree-level contribution to the 2-point function is shown in Fig. S3 and is trivially $\alpha_{\rm NP}/m_\phi^2$. In the EFT, a similarly simple calculation produces C/m_ϕ^2 for the two-point function. As expected, at tree level the matching gives

$$C_{\rm tree} = \alpha_{\rm NP} \tag{S15}$$

Still at LO in NP, we can calculate to an additional order in the QED coupling α which arrises at one loop and is also shown in Fig. S3. Since Coulomb scattering diverges as the incoming velocity goes to zero, we will not be surprised to encounter an IR divergence in this calculation. However, as expected, the IR divergence has an identical structure in the full and effective theories and will thus not affect the value of the Wilson coefficient at order α. In the full theory we find the two point function

$$\text{Full theory:} \qquad D_{ee}^{(1)} = \int \frac{d^3q}{(2\pi)^3}\,\frac{\alpha_{\rm NP}}{q^2+m_\phi^2}\,\frac{1}{E-\frac{q^2}{2m_e}}\,\frac{Z_{\rm eff}e^2}{q^2+\lambda^2} \sim -\frac{2\alpha_{\rm NP}Z_{\rm eff}\alpha m_e}{\lambda m_\phi^2} + \frac{2\alpha_{\rm NP}\,Z_{\rm eff}\alpha m_e}{m_\phi^3} + \dots \tag{S16}$$

where the three terms in the integrand are the Yukawa, electron and Coulomb propagator, respectively, and we used $\alpha = e^2/4\pi$ and $E = 0$. The coulomb potential is IR-regulated by λ. The result in Eq. (S16) has been expanded at large m_ϕ. The second term in Eq. (S16) is already reminiscent of the m_ϕ^{-3} term in Eq. (S14). Repeating the $O(\alpha)$ computation in the EFT is straightforward,

$$\text{EFT:} \qquad D_{ee}^{(1)} = \int \frac{d^3q}{(2\pi)^3}\,\frac{C}{m_\phi^2}\,\frac{1}{E-\frac{q^2}{2m_e}}\,\frac{Z_{\rm eff}e^2}{q^2+\lambda^2} \sim -\frac{2CZ_{\rm eff}\alpha m_e}{\lambda m_\phi^2}\,. \tag{S17}$$

As expected, using the tree-level value for C, Eq. (S15), the IR divergences in the full and effective theories match at order α. However, the second term in Equation (S16), leads to a finite correction to the Wilson coefficient at $O(\alpha)$,

$$\Delta C = \frac{2\alpha_{\rm NP}Z_{\rm eff}\alpha m_e}{m_\phi} = \frac{2\alpha_{\rm NP}Z_{\rm eff}}{a_0 m_\phi}\,. \tag{S18}$$

We thus find that the 1-loop correction to the m_ϕ^{-2} Wilson coefficient shown in Fig. S3 leads to an effective operator which scales as $Z_{\rm eff}/(a_0 m_\phi)^3$, in qualitative agreement with our position-space calculation. The two calculations are related. The position space calculation makes use of the hydrogen wavefunction and thus in some sense re-sums diagrams with an arbitrary number of photon exchanges between the nucleus and the electron before and after the scalar line. The EFT calculation isolates the first of these corrections. In both calculations we have accounted for multi-electron effects by taking the nuclear charge to be an effective one, with the potential being Coulombic otherwise. Again, we find that the mismatch between the $Z_{\rm eff}$'s does not allow this term to be absorbed in the FS.

We are, however, not surprised that the numerical coefficients of the m_ϕ^{-3} terms in Eqs. (S14) and (S18) do not agree since the former captures bound state dynamics, properly resumming IR effects that are dominant at the Bohr radius.

---

[1] D. Budker, D. DeMille, E. D. Commins, and M. S. Zolotorev, "Experimental investigation of excited states in atomic dysprosium," *Phys. Rev.* **A50** (Jul, 1994) 132–143. http://link.aps.org/doi/10.1103/PhysRevA.50.132.

[2] N. Leefer, L. Bougas, D. Antypas, and D. Budker, "Towards a new measurement of parity violation in dysprosium," 2014. arXiv:1412.1245 [physics.atom-ph].

[3] V. A. Dzuba, V. V. Flambaum, and M. G. Kozlov, "Combination of the many-body perturbation theory with the configuration-interaction method," *Phys. Rev.* **A54** (1996) 3948.

[4] J. C. Berengut, V. A. Dzuba, and V. V. Flambaum, "Isotope shift calculations for atoms with one valence electron," *Phys. Rev.* **A68** (2003) 022502, arXiv:physics/0305068 [physics].

[5] J. C. Berengut, V. V. Flambaum, and M. G. Kozlov, "Calculation of isotope shifts and relativistic shifts in CI, CII, CIII and CIV," *Phys. Rev.* **A73** (2006) 012504, arXiv:physics/0509253 [physics].

[6] W. R. Johnson, S. A. Blundell, and J. Sapirstein, "Finite basis sets for the dirac equation constructed from B splines," *Phys. Rev.* **A37** (Jan, 1988) 307–315. http://link.aps.org/doi/10.1103/PhysRevA.37.307.

[7] V. M. Shabaev, I. I. Tupitsyn, V. A. Yerokhin, G. Plunien, and G. Soff, "Dual kinetic balance approach to basis-set expansions for the dirac equation," *Phys. Rev. Lett.* **93** (Sep, 2004) 130405. http://link.aps.org/doi/10.1103/PhysRevLett.93.130405.

[8] J. C. Berengut, "Particle-hole configuration interaction and many-body perturbation theory: Application to Hg^+," *Phys. Rev.* **A94** (2016) 012502.

[9] P. Jonsson, G. Gaigalas, J. Biero, C. F. Fischer, and I. Grant, "New version: GRASP2K relativistic atomic structure package," *Computer Physics Communications* **184** (2013) no. 9, 2197 – 2203. http://www.sciencedirect.com/science/article/pii/S0010465513000738.

[10] C. Delaunay, R. Ozeri, G. Perez, and Y. Soreq, "Probing Atomic Higgs-like Forces at the Precision Frontier," *Phys. Rev.* **D96** (2017) no. 9, 093001, arXiv:1601.05087 [hep-ph].

[11] W. E. Caswell and G. P. Lepage, "Effective Lagrangians for Bound State Problems in QED, QCD, and Other Field Theories," *Phys. Lett.* **167B** (1986) 437–442.

[12] R. J. Hill, G. Lee, G. Paz, and M. P. Solon, "NRQED Lagrangian at order $1/M^4$," *Phys. Rev.* **D87** (2013) 053017, arXiv:1212.4508 [hep-ph].

[13] T. Kinoshita and M. Nio, "Radiative corrections to the muonium hyperfine structure. 1. The $\alpha^2(Z\alpha)$ correction," *Phys. Rev.* **D53** (1996) 4909–4929, arXiv:hep-ph/9512327 [hep-ph].